J. Biochem. 2012;152(1):73–85 doi:10.1093/jb/mvs034

JB THE JOURNAL OF BIOCHEMISTRY

Mitochondrial P5, a member of protein disulphide isomerase family, suppresses oxidative stress-induced cell death

Received January 5, 2012; accepted March 15, 2012; published online April 4, 2012

Yu Shitara, Yuichi Tonohora, Takahiro Goto, Yasuhiro Yamada, Takashi Miki, Hirokazu Makino, Masanao Miwa and Tohru Komiya*

Faculty of Bioscience, Nagahama Institute of Bioscience and Technology, Nagahama, 526-0829, Japan

*Tohru Komiya. Faculty of Bioscience, Nagahama Institute of Bioscience and Technology, Nagahama, 526-0829, Japan. Tel: +81 0749 64 8106, Fax: +81 0749 64 8140, email: t_komiya@nagahama-i-bio.ac.jp

P5, one of the protein disulphide isomerase (PDI) family members, catalyses disulphide bond formation in proteins and exhibits molecular chaperone and calcium binding activities *in vitro*, whereas its physiological significance remains controversial. Recently, we have reported that P5 localizes not only in the ER but also in mitochondria, although it remains unclear so far about its physiological significance(s) of its dual localization. Here we report that H_2O_2− or rotenone-induced cell death is suppressed in MTS-P5 cells, which stably express P5 in mitochondria. H_2O_2-induced cell death in Saos-2 cells occurred, in large part, through caspase-independent and poly(ADP-ribose) polymerase (PARP)-dependent manner. In MTS-P5 cells challenged with H_2O_2 treatment, PARP was still activated, whereas release of cytochrome *c* or apoptosis-inducing factor and intramitochondrial superoxide generation were suppressed. We also found that mitochondrial P5 was in close contact with citrate synthase and maintained large parts of its activity under H_2O_2 exposure. These results suggest that mitochondrial P5 may upregulate tricarboxylic acid cycle and possibly, other intramitochondrial metabolism.

Keywords: cell death/mitochondria/oxidative stress/PARP/PDI.

Abbreviations: AIF, apoptosis-inducing factor; cyt *c*, cytochrome *c*; ER, endoplasmic reticulum; F1β; FoF1-ATPase subunit β; hsp60, heat shock protein 60; hsp70, heat shock protein 70; IMS, intermembrane space; MOMP, mitochondrial outer membrane permeabilization; PARP, poly(ADP-ribose) polymerase; PDI, protein disulphide isomerase.

Protein disulphide isomerase (PDI) (EC5.3.4.1) is a key enzyme responsible for the oxidation, reduction and isomerization of disulphide bonds in proteins in the endoplasmic reticulum (ER) (*1*, *2*). PDI and related proteins constitute a protein family (*1*, *2*) and have two or three CGHC sequences in their active sites. P5, one of PDI family members, catalyses disulphide bond formation and its isomerization and exhibits molecular chaperone and calcium binding activities *in vitro*, whereas its physiological significance remains controversial (*3*–*6*). Like many other soluble PDI family members in the ER, P5 contains both the secretory signal sequence at its amino-terminus and the ER retrieval signal at its carboxy-terminus and is indeed mostly localized in the ER lumen (*7*). Recently, we have reported that P5 localizes not only in the ER but also in the mitochondria (*8*), although it remains unclear so far about its physiological significance(s) of its dual localization.

Mitochondria are intracellular powerhouse, which produce adenosine 5′ triphosphate (ATP) through the concerted action of the enzymes for tricarboxylic acid (TCA) cycle and the respiratory chain complexes. Recent extensive studies show that the organelles are also the major executioner in some cell death programmes (*9*, *10*). The caspase-dependent cell death pathways are well characterized and classically categorized into the 'intrinsic', mitochondrial and the 'extrinsic', death receptor pathways (*9*, *10*). In the intrinsic pathway, upon death-inducing stimuli proapoptotic Bcl-2-related proteins like Bax or Bak are activated and concomitantly mitochondrial outer membrane permeabilization (MOMP) is induced to release several intramitochondrial proteins, such as cytochrome *c*, Smac/DIABLO, HtrA2/Omi, apoptosis-inducing factor (AIF), several of which are involved in the caspase activation cascades, eventually leading to cell demise (*9*, *10*). Recent reports indicate that cell death is induced even in a caspase-independent manner, and some of such types of cell death have been characterized so far. Among these are the autophagic cell death, necroptosis and poly(ADP-ribose) polymerase (PARP)-dependent cell death, in all of which much remains to be characterized (*10*, *11*). Notably, many studies of these caspase-independent cell death have been performed under caspase-inactivated conditions, for example, in Bax/Bak-double knockout cells, suggesting that these cell death pathways may be back-up system in case for caspase inactivation, though many of their physiological significance(s) are not yet clear (*10*, *11*).

Reactive oxygen species (ROS) such as superoxide anion and hydrogen peroxide (H_2O_2) are not only known to act as critical signalling molecules but also trigger cellular dysfunction by damaging lipids, proteins, nucleic acids and so on (*12*–*15*). Intracellular levels of ROS are strictly regulated by superoxide dismutase (SOD), the glutathione system and the thioredoxin system that can detoxify them (*12*–*14*).

Oxidative stress occurs when the levels of ROS overwhelm these antioxidant defence systems, leading to activation of stress signalling pathways or even to cell death by apoptosis or necrosis (*15*). H_2O_2 is a relatively stable ROS and acts both a mediator of cytotoxicity and a signalling molecule in living cells (*12*, *13*, *16*). The major forms of oxidative DNA damage are lesions such as 8-oxo-2′deoxyguanosine that are repaired by base excision repair including PARP activation (*17*). Recent studies show that H_2O_2 induces cell death in PARP-dependent manner, though how 'live or die' decision is made is not well understood yet (*18*, *19*). On the other hand, rotenone, an inhibitor of complex I to generate ROS, is reported to cause apoptosis, though how rotenone triggers apoptosis is still an unresolved issue (*20–24*).

In the present study, to elucidate the physiological function(s) of P5 in mitochondria, we have made a transformant, which stably expressed P5 in mitochondria and characterized it with respect to the effect on oxidative stress-induced cell death.

Experimental Procedures

cDNA cloning of mouse P5 and constructions of MTS-P5

The cDNA encoding the mouse P5 (accession No. NM_027959) was prepared by RT–PCR using P19 cells' poly(A)$^+$ RNA as a template and the following primers: mP5N1, mP5C1, mP5N2 and mP5C2 (Supplementary Table SI). PCR fragments were subcloned into pGEM-T Easy vector (Promega) or pBluescript II SK (+) vector (Stratagene), and the full-length cDNA was obtained using its endogenous restriction sites. The cDNA clone of FLAG-tagged P5 mature region was prepared by PCR using full-length cDNA as a template and the following primers: mP5N6/ECO/NDE, mP5C3/FLAG/SAL and mP5C4/FLAG/SAL (Supplementary Table SI). mP5N6/ECO/NDE and mP5C1 were used to delete the original signal sequence portion and mP5C3/FLAG/SAL and mP5C4/FLAG/SAL were used to insert the FLAG tag sequence in front of the KDEL sequence. MTS region was prepared by PCR using full-length cDNA of OXA1 (accession No. NM_026936) as a template and the following primers: mOXA1N1/BAM and mOXA1C3/ECO (Supplementary Table SI). In-frame cDNA clone of MTS-P5 was obtained from resultant two PCR fragments using their restriction sites and subcloned into the mammalian cell expression vector pcDNA3 (Invitrogen).

Cell cultures

Saos-2 or MTS-P5 cells were cultured in DMEM containing 10% (v/v) fetal calf serum, 4 mM L-glutamine, 0.2% (w/v) $NaHCO_3$, 100 U/ml penicillin and 100 μg/ml streptomycin at 37°C in a 5% CO_2 incubator.

Screening for the stable transformants of MTS-P5

For stable expression, MTS-P5 plasmids were first linearized with NruI and then transfected into Saos-2 cells by using lipofectamine reagent (Invitrogen). After single colonies were isolated, cells were screened in the presence of G418 (Sigma) at the concentration of 1.6 mg/ml.

Subcellular fractionation, proteinase-sensitivity assay and hypotonic treatment

Cells grown on 10-cm dish were washed once with cold PBS, collected and suspended into the 'HEMS buffer' containing 10 mM HEPES–KOH (pH 7.4), 1 mM EDTA, 220 mM mannitol, 70 mM sucrose and one Complete EDTA-Free tablet (Roche). Cells were then homogenized through 20 G syringe 20–30 times and the homogenates were applied to conventional subcellular fractionation as described previously (*8*). Briefly, the pellets from the 8,000*g* centrifugation were washed with excess amounts of HEMS buffer to obtain the heavy membrane (crude mitochondria) fraction and the supernatants were subjected to ultracentrifugation at 100,000*g* for 60 min at 4°C to obtain the microsomal and cytosolic fractions. Each sample obtained above was subjected to SDS–PAGE followed by western blot analysis using the antibodies indicated in the figures. For protease-sensitivity assay mitochondria (10 μg) were treated with proteinase K at the concentrations indicated in the figures as described previously (*25*) except using HEMS buffer. Hypotonic treatment was performed as described (*8*). Detection was performed by ECL or ECL-plus (GE Healthcare) and analysed by LAS-1000 plus or LAS-4000 (GE Healthcare). Protein concentrations were determined with a BCA assay kit (Pierce).

Immunofluorescence microscopy

Saos-2 cells or MTS-P5 cells (5×10^4 cells) were first cultured on coverslips for 24 h, then incubated with 100 nM MitoTracker Red (Molecular Probes) for 15 min. After rinsed with 1× PBS briefly, they were fixed with 4% (w/v) paraformaldehyde (PFA) for 15 min, treated with methanol/acetate (50%/50%, v/v) for 3 min at room temperature. After rinsed with 1× PBS briefly, they were incubated with 1× PBS containing 5% goat serum for 30 min at room temperature, and further treated with the primary antibodies indicated in the figures for 60 min, followed with the secondary antibodies conjugated with Alexa568 (Molecular Probes) or FITC (BIOSOURCE). Nuclei were stained with Hoechst 33342. Labelled cells were observed with a confocal laser-scanning microscope (FluoView FV1000, Olympus) and analysed with FV10-ASW software (Olympus). In order to check the release of mitochondrial death-inducing factors, each cell was pretreated with 500 μM H_2O_2.

Cell viability assays

The cell viability was measured by trypan blue exclusion assay or XTT (sodium 3′-[1-[(phenylamino)-carbonyl]-3,4-tetrazolium]-*bis*(4-methoxy-6-nitro)-benzene-sulphonic acid hydrate) assay (Cell proliferation kit ll, Roche). For trypan blue exclusion assay cultured cells (5×10^4 cells/well) on six well plates were treated with the reagents described in the figures. Both cultured medium and cells on the plates were collected separately, centrifuged at 3,000 rpm for 10 min by

swing rotor (himac CT6D, Hitachi). The pellets were resuspended in PBS, mixed with the same amount of trypan blue solution and viable and non-viable cells were then counted. For XTT assay, cells were seeded in triplicate onto 96-well plates at 1×10^4 cells/well. Plates were analysed in a microtiter plate reader (Biotrak II plate reader, Amersham) at 492 nm with a reference of 620 nm. Viability was shown by relative values to those of control cells regarding as 100%. Data were shown by mean ± SD and statistical analysis was performed using Student's *t*-test.

siRNA transfection

The following Stealth RNA duplexes (Invitrogen) were used for knockdown experiments.

AIF sense; 5′-GGAGUCAGCAGUGGCAAGUU ACUUA-3′.

AIF antisense; 5′-UAAGUAACUUGCCACUGCU GACUCC-3′.

Stealth RNAi negative control duplexes (Invitrogen) whose GC content is similar to that of each duplex siRNA were used as 'scrambled' negative controls. Cells were grown to 40–50% confluence on a 6-well plate and transfected with siRNAs shown above (100 pmol each) using Lipofectamine 2000 (Invitrogen). After 48 h, cells were retransfected as above for 24 h and used in the experiments.

Flow cytometry analysis

Mitochondrial membrane potential ($\Delta\Psi$m) was analysed using JC-1 (AAT Bioquest). Cells were first treated with 2.5 μg/ml of JC-1 for 30 min at 37°C, collected, washed three times with cold PBS. The fluorescence intensities were measured using a flow cytometer at FL1 and FL2 channels (JSAN desktop cell sorter, Bay Bioscience). The data were analysed using AppSan software (Bay Bioscience) and shown by FL2/FL1 ratio. Mitochondrial superoxide generation was analysed using MitoSOX Red (Molecular Probes). Cells were first treated with 5 μM MitoSOX Red for 15 min at 37°C, collected, washed three times with PBS. The fluorescence intensity was measured using the flow cytometer at FL2 channel with counting 5,000 cells for each sample.

Crosslinking and immunoprecipitation

Isolated mitochondria (200 μg) were treated with 5 mM DSP (Pierce), a cleavable cross-linking reagent, for 30 min at room temperature. After quenched with 100 mM Tris–HCl (pH 8.0) for 15 min at room temperature, the cross-linked adducts were washed once with HEMS buffer, centrifuged at 16,100*g* for 5 min at 4°C. The pellets were then treated with lysis buffer (10 mM HEPES–KOH, pH 7.4, 2 mM EDTA, 150 mM NaCl, and 1% (w/v) Triton X-100) for 30 min on ice. After adding the washing buffer [10 mM HEPES–KOH, pH 7.4, 2 mM EDTA, 150 mM NaCl and 0.05% (w/v) Triton X-100], the extracts were cleared by centrifugation for 30 min at 100,000*g* at 4°C. The resulting supernatants were incubated at 4°C overnight with the anti-FLAG M2-agarose beads (Sigma). After centrifuged at 800*g* for 5 min, the beads were washed twice in HEMS buffer and the supernatants were precipitated by 10% (w/v) trichloroacetic acid. Each sample obtained above was incubated at 37°C for 30 min in SDS–PAGE loading buffer containing 20 mM DTT to cleave DSP and subjected to SDS–PAGE followed by western blot analysis.

Measurement of citrate synthase activity

Citrate synthase activity was analysed using isolated mitochondria described above. Briefly, mitochondria (10 μg) were first added to the reaction buffer containing 100 mM Tris–HCl (pH 8.0), 100 μM 5,5′-dithiobis-(2-nitrobenzoic acid) (DTNB), 50 μM acetyl coenzyme A and 0.1% (w/v) Triton X-100 and the reaction was started by addition of 250 μM oxaloacetate. The activity was measured as the increase in absorbance at 412 nm using SmartSpec Plus spectrophotometer (BIO-RAD).

Antibodies

Antibodies used in this work are: FLAG (Sigma), $F_1\beta$ (BD Biosciences), calnexin (Santa Cruz), hsp70 (Santa Cruz), hsp60 (BD Biosciences), procaspase-3 (Santa Cruz), PARP-1 (Santa Cruz), Tom20 (Santa Cruz or BD Biosciences), cytochrome *c* (Santa Cruz or BD Biosciences), AIF (Santa Cruz or Cell Signaling), Smac/DIABLO (Stressgen or BD Biosciences), HtrA2/Omi (R&D), citrate synthase (Nordic Immunology), PDI (BD Biosciences), actin (Santa Cruz). Rabbit anti-P5 antibodies were raised against *Escherichia coli*-expressed human P5 and affinity purified. Anti-10H monoclonal antibodies were prepared as described previously (*26*).

Results

Oxidative stress-induced cell death is suppressed in the cells which express mitochondrially localized P5

Previously, we have shown that P5 is localized not only in the ER, but also in mitochondria (*8*). To understand physiological role(s) of mitochondrial P5, we first made cell lines in which P5 proteins were stably expressed in mitochondria (termed 'the MTS-P5 cells') using Saos-2 osteosarcoma cells as a donor, because in these cells mitochondria show normal morphology and mitochondrial mass, and they are often used in studying cell death (*27*). Since the mitochondrial targeting signal (MTS) portion of endogenous P5 has not yet been clearly defined, we have made the clone that consists of mature portion of P5 fused both to MTS of mouse Oxa1 instead of its signal sequence at amino-terminal and to FLAG tag before carboxy-terminal KDEL ER retrieval signal (termed 'MTS-P5-FLAG', see Fig. 1A). After isolating the MTS-P5 cells, as shown in Fig. 1B and C, the expressed fusion protein in these cells was indeed localized to mitochondria. The expression level of mitochondrial P5 in MTS-P5 cells was around 3-fold compared to that in control, Saos-2 cells (Supplementary Fig. S1A). As shown in Supplementary Fig. S1B, the expressed protein in MTS-P5 cells was cofractionated with the pellets (the mitoplasts) after hypotonic treatment, while some fractions of endogenous P5 were collected in the supernatants, suggesting a fraction of it

localizes in the intermembrane space. As also shown in Supplementary Fig. S1C, the proteinase K-sensitivity of the expressed protein was much similar to that of hsp60 (the matrix protein) whose significant portions were resistant at 100 μg/ml of proteinase K, whereas not to those of Tom20 (the outer membrane protein) whose large portions were sensitive at 0.5 μg/ml of proteinase K, or to those of AIF (the inner membrane protein exposed its large portion to the intermembrane space) whose significant portions were degradable at 10 μg/ml of proteinase K to smaller sizes (Supplementary Fig. S1C, single asterisk of AIF panel). As also shown in the figure is that the expressed protein was not localized in microsomes [Supplementary Fig. S1C, FLAG (Ms) panel]. These results show that the most portions of the expressed protein reside in the mitochondrial matrix as expected, because the fused MTS portion should target passenger protein to mitochondrial matrix. In contrast, while most fractions of the endogenous P5 were resistant at 100 μg/ml of proteinase K, even at above this

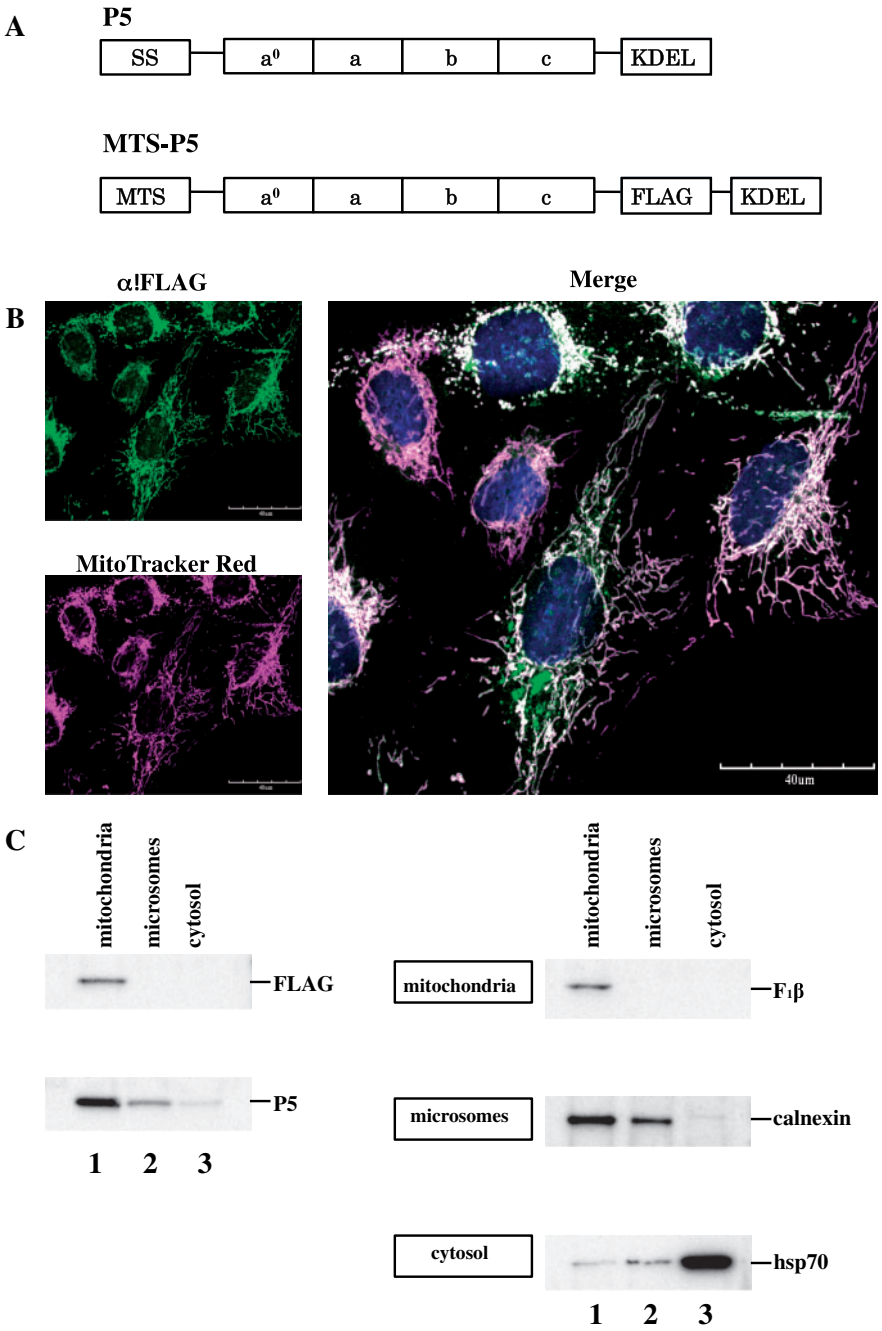

Fig. 1 Intracellular localization of MTS-P5. (A) Schematic diagrams of domain structure of original P5 and MTS-P5. SS: signal sequence, a^0, a^0 domain containing catalytic CGHC motif; a, a domain containing catalytic CGHC motif; b, b domain; c, c domain containing acidic Ca^{2+} binding activity; KDEL, C-terminal ER retrieval motif; MTS, mitochondrial targeting signal. (B) Immunofluorescent microscope images of MTS-P5 cells. MTS-P5 cells were stained with anti-FLAG antibody (green), MitoTracker Red (magenta) and Hoechest 33342 (blue) and then observed by a confocal laser scanning microscope. Bar indicates 40 μm. (C) Subcellular fractionation of MTS-P5 cells. MTS-P5 cells were fractionated as described in 'Experimental Procedures' section and the resulting mitochondrial (lane 1), microsomal (lane 2) and cytosolic (lane 3) fractions were subjected to SDS–PAGE followed by western blotting using antibodies indicated in the figure.

concentration some portions were also resistant. This is probably due to microsomal contamination because microsomal P5 was resisitant to even at 1,500 μg/ml of proteinase K [Supplementary Fig. S1C, P5 (Ms) panel].

Using the cell clones thus obtained, we next examined any effects on cell death induced by oxidative stress using the trypan blue exclusion assay (Fig. 2). As shown in Fig. 2A and B, H_2O_2 induced cell death in a dose- and time-dependent manner, while such cell death was effectively suppressed in the MTS-P5 cells. It should be noted that in our assays Saos-2 cells are rather resistant to H_2O_2 because ~90% of them are likely to be alive even at 200 μM, the concentration of which many cell types cause apoptosis (Fig. 2A). Cell death suppression was also observed with rotenone, the ROS generating reagent by inhibiting mitochondrial respiratory complex I electron transport activity (Fig. 2C and D). Essentially the same results were obtained with the MTS-P5 clone made with HeLa cells (Y. Tonohora *et al.*, unpublished data). We hereafter performed experiments on H_2O_2-induced cell death pathway.

H_2O_2-induced cell death is poly(ADP-Ribose) polymerase (PARP) dependent

Next, we examined what mechanisms caused H_2O_2-induced cell death in the wild-type Saos-2 cells. As shown in Fig. 3A, using the XTT assay, it was hardly suppressed by the pretreatment with z-VAD.fmk, the pan-caspase inhibitor [Fig. 3A(a)], whereas effectively with DPQ (3,4-dihydro-5-[4-(1-piperidinyl)butoxyl]-1(2H)-isoquinolinone), the poly(ADP-ribose) polymerase (PARP) inhibitor [*28*; Fig. 3A(b)]. Notably, the viability measured with the XTT assay was apparently much lower than that with the trypan blue exclusion assay for unknown reason. In sharp contrast, staurosporine (STS), the well-known inducer of caspase-dependent cell death, induces cell death that was effectively suppressed by z-VAD.fmk (Fig. 3Ba), but not by DPQ [Fig. 3B(b)]. By further assays, we revealed that H_2O_2-induced cell death was significantly suppressed with the antioxidant, *N*-acetyl L-cysteine (NAC), but not with cyclosporine A (inhibitor of permeability transition pore), 3-methyladenine (inhibitor of autophagy), MDL28170 (calpain inhibitor) or necrostatin-1 (*29*; necroptosis inhibitor) (Table I). These results suggest that in Saos-2 cells H_2O_2 (500 μM) induces cell death mainly in a PARP-dependent manner even without inactivation of Bax and Bak.

Previous reports showed that in the PARP-mediated cell death pathway mitochondrial intermembrane space proteins such as cytochrome *c* and AIF are released into the cytosol (*28*, *30*). In order to check this, we next performed the experiments using immunofluorescence microscopy and cell fractionation

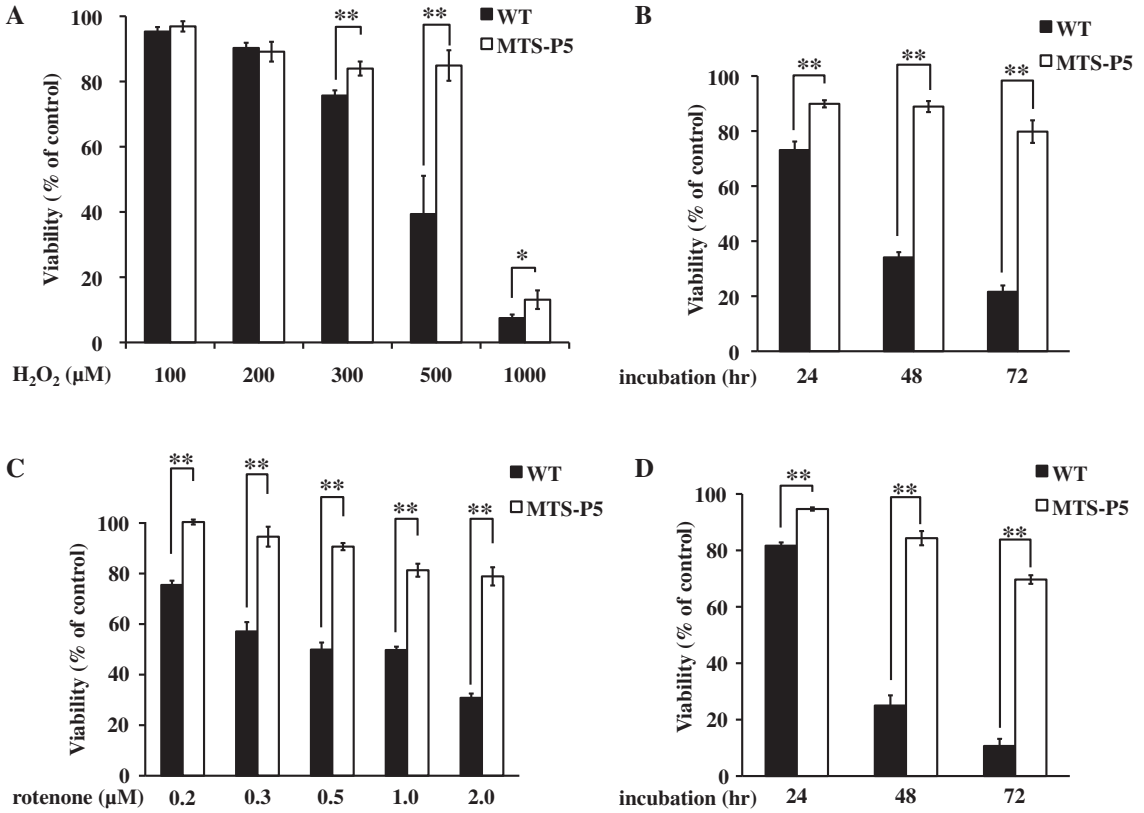

Fig. 2 Oxidative-stress-induced cell death is suppressed in MTS-P5 cells. (A) H_2O_2 -induced cell death is suppressed in MTS-P5 cells in a dose-dependent manner. Saos-2 or MTS-P5 cells were first cultured on six well plates for 24 h and then treated with H_2O_2 for 48 h at concentrations indicated in the figure. The cell viability was measured by trypan blue exclusion assay and indicated as described in 'Experimental Procedures' section ($n=6$). (B) Time course of H_2O_2-induced cell death. Cells were treated with 500 μM H_2O_2 for the indicated times. ($n=4$). (C) Rotenone-induced cell death is suppressed in MTS-P5 cells. Cells were treated with rotenone at the indicated concentrations ($n=3$). (D) Time course of rotenone-induced cell death. Cells were treated with 2 μM rotenone for the indicated times ($n=3$). The single and double asterisks indicate $P<0.05$ and $P<0.01$, respectively.

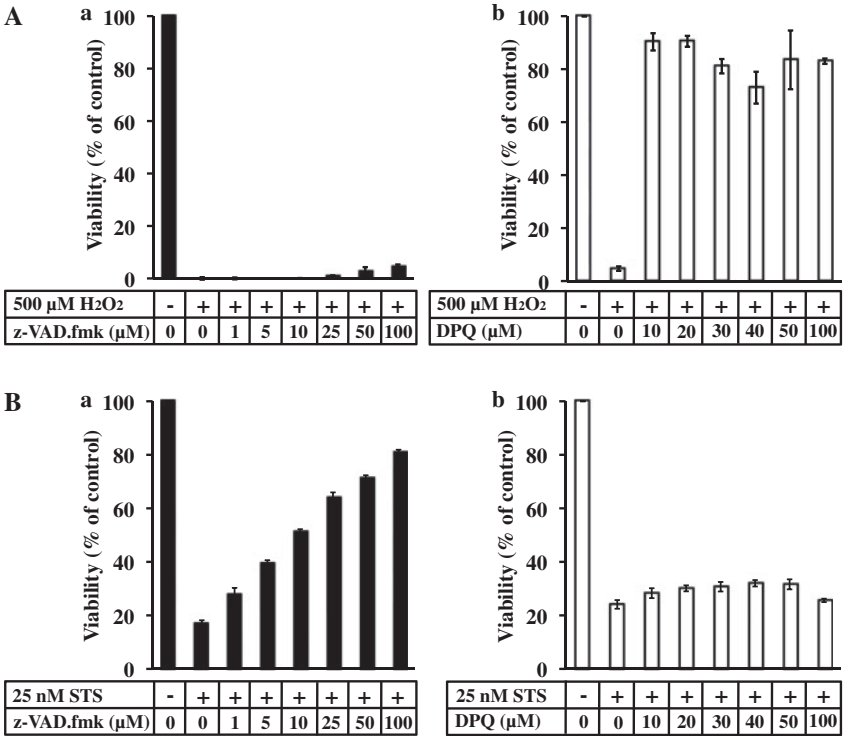

Fig. 3 H_2O_2-induced cell death is PARP dependent, but caspase independent in Saos-2 cells. Saos-2 cells were pretreated with indicated concentration of DPQ (a) or z-VAD.fmk (b) for 1 h before 500 μM H_2O_2 (A) or 25 nM staurosporine (STS) (B) treatment. After 48 h cell viability was measured by XTT assay as described in 'Experimental Procedures' section ($n = 3$).

Table I. Summary of the effects of reagents on H_2O_2– or staurosporine (STS)-induced cell death.

Reagents	H_2O_2 (500 μM)	STS (25 nM)
z-VAD.fmk (100 μM)	–	+
DPQ (30 μM)	+	–
cyclosporine A (5 μM)	–	–
N-acetyl L-cysteine (10 mM)	+	+
3-methyladenine (10 mM)	–	ND
MDL28170 (50 μM)	–	ND
necrostatin-1 (30 μM)	–	ND

+, cell death is suppressed; –, cell death is not suppressed; ND, not determined.

experiments. As shown in Fig. 4A, upon H_2O_2 treatment for 8 h, cytochrome *c* was released from mitochondria to the cytosol. Release was also indicated by inconsistent distribution patterns of fluorescence intensity (Fig. 4B). Similar release was observed for Smac/DIABLO (Supplementary Fig. S2A), HtrA2/Omi (Supplementary Fig. S2B), while less frequently for AIF (Fig. 4C), judging also from the inconsistent distribution patterns of AIF with those of Tom20 (Fig. 4D). In the cell fractionation experiments, we detected the release of not only cytochrome *c*, but also AIF, probably in the processed form in the cytosol (asterisks in the figure), though less than the formers in amount (Fig. 4E). These results suggest that in our study AIF is released less effectively than observed with the other factors upon H_2O_2 treatment. We also obtained the results that the release of cytochrome *c* and AIF was suppressed by DPQ, but not by z-VAD.fmk with both immunofluorescence microscopy (Supplementary Fig. S3A–D) and the cell fractionation experiments (Supplementary Fig. S3E), consistent that PARP activation is necessary for the release.

In H_2O_2-induced cell death AIF plays an important role

The results shown above suggest that in Saos-2 cells H_2O_2-induced cell death occurs without caspase activation though cytochrome *c* is released. Since in some of the previous studies H_2O_2 is known to induce the caspase dependent, intrinsic pathway, we next examined whether caspase-9 and caspase-3 are activated in H_2O_2-treated Saos-2 cells. While the processing forms of procaspase-3 and PARP-1 were clearly detected in STS-treated cells (Fig. 5A), they were negligibly detected in H_2O_2-treated ones (Fig. 5B), consistent with our previous data (Fig. 3A). This seemingly caspase-independent cell death is induced without the activity of HtrA2/Omi because Ucf-101, the inhibitor of HtrA2/Omi serine protease activity, did not significantly affect on it (*31*; Supplementary Fig. S4). Although we do not exclude the possibility that HtrA2/Omi is required for the H_2O_2-induced cell death in Saos-2 cells since in the previous studies the serine protease activity of HtrA2/Omi is required for caspase-independent cell death, we consider it less likely at present (*32*, *33*).

Next, we checked whether AIF, another candidate for caspase-independent cell death executioner, is required for the H_2O_2-induced cell death using siRNA that is designed to knockdown human AIF.

We first checked several siRNAs and then selected only one candidate that not only knocked down AIF but also kept cells alive, because the rest siRNAs were lethal under our experimental conditions (Y. Shitara *et al*., data not shown). As shown in Fig. 5C, using this siRNA expression of endogenous AIF was effectively suppressed. Under these conditions, trypan blue exclusion assay was performed after treatment with H_2O_2. As shown in Fig. 5D, death was significantly compromised with AIF knockdown compared with control, although the viability measured with control, scrambled siRNA was apparently higher than that with the previous data in Fig. 2A for unknown reason. Taken together, the results shown above suggest that in Saos-2 cells H_2O_2 induces cell death in PARP-dependent and caspase-independent manner and that AIF, probably not HtrA2/Omi, plays an important role for cell death induction, even though the amount of release is negligible compared with that of cytochrome *c*. Notably we do not exclude the possibility that some other factor(s) other than AIF are required, because the cell death was not completely suppressed by the knockdown (Fig. 5D).

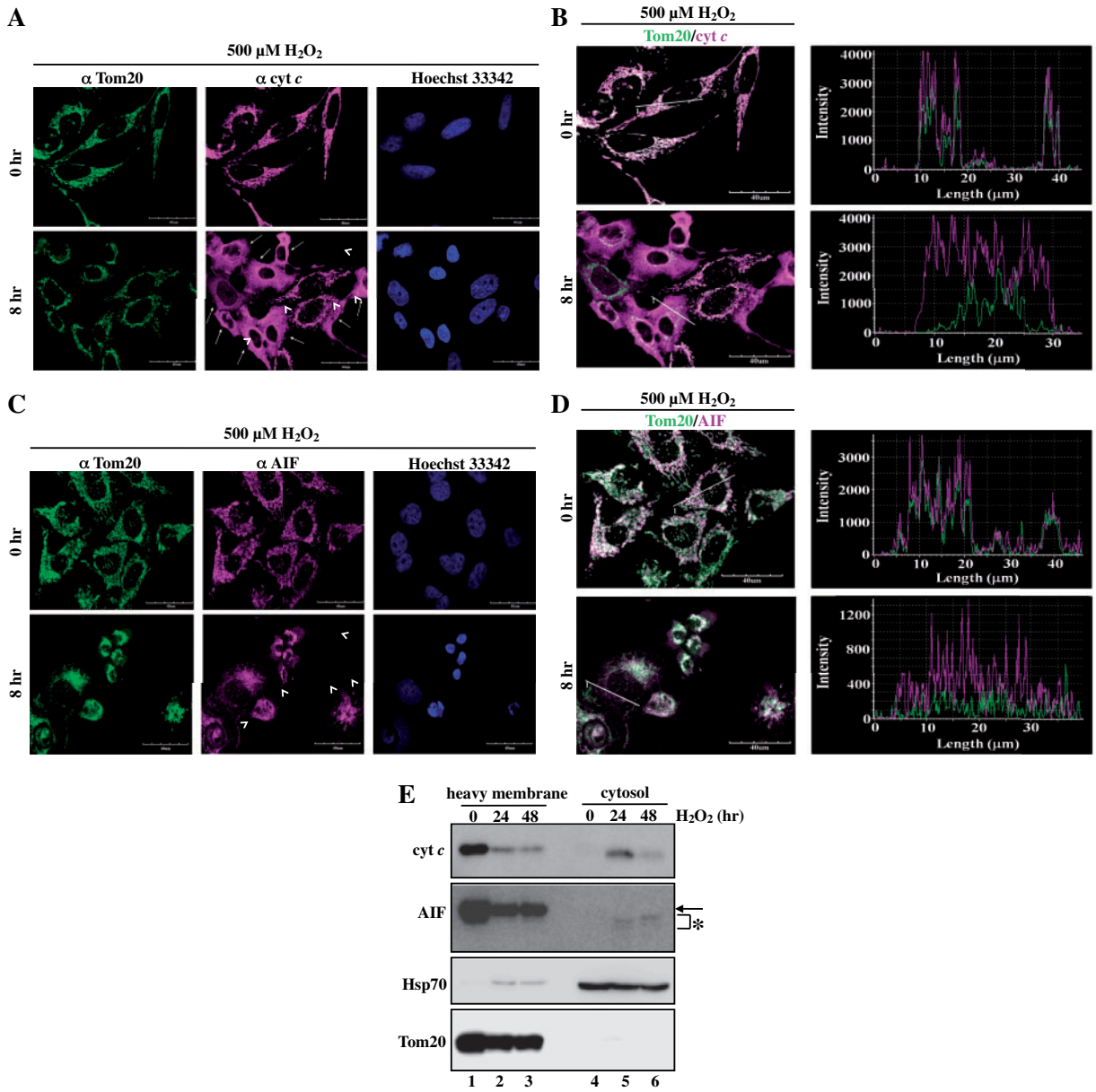

Fig. 4 Intramitochondrial cell death-inducing factors are released upon H_2O_2 treatment. (A and C) Saos-2 cells were treated with 500 μM H_2O_2 for 8 h and then stained using antibodies against Tom20 (green), cyt *c* (A) or AIF (C) (magenta) and with Hoechest 33342 (blue). Cells were observed with confocal microscopy. Arrows indicate the cells in which cell death-inducing factors are released. Bar indicates 40 μm. (B and D) (left) The images of Tom20 and cyt *c* (A) or AIF (C) were merged and shown in (B) or (D), respectively. (Right) Intracellular distribution of Tom20 and cyt *c* (B) or AIF (D) indicated by fluorescence intensity when sectioned at a line in each merged panel. (E) Release of cell death-inducing factors revealed by subfractionation followed by western blotting analysis. Cells were treated with 500 μM H_2O_2 for indicated times and then fractionated to obtain heavy membrane and cytosol fractions. Each fraction was subjected to SDS–PAGE followed by western blotting analysis using antibodies against cyt *c*, AIF, Tom20 and Hsp70. Arrow indicates mature AIF and asterisk indicates truncated form of AIF.

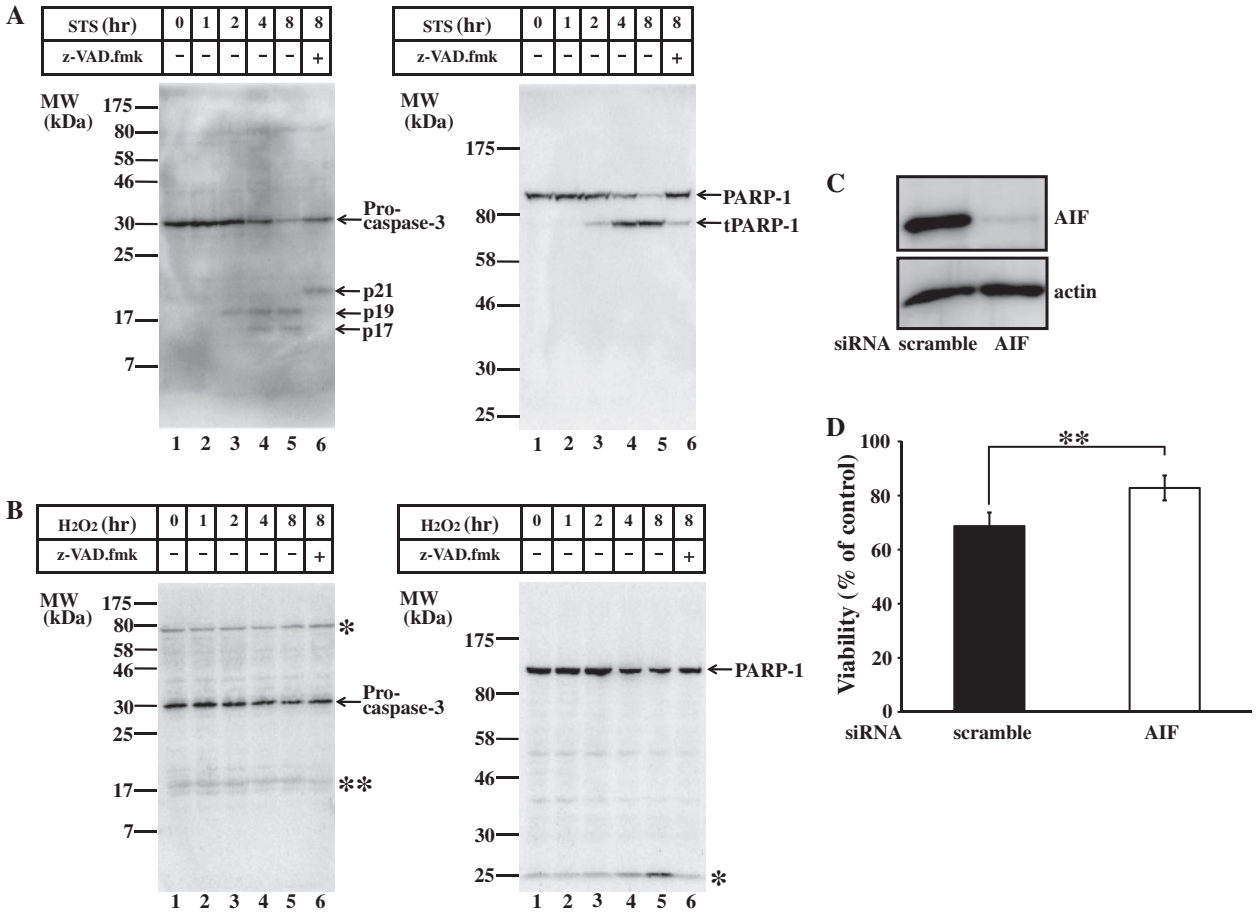

Fig. 5 Upon H_2O_2 treatment processed forms of caspase-3 and PARP are negligibly detected and in this pathway AIF is an important factor. (A) Both caspase-3 and PARP are efficiently processed upon STS treatment. Saos-2 cells were treated with 1 μM staurosporine (STS) for indicated times in the presence or absence of z-VAD.fmk (100 μM). Then each reaction was stopped with 10% (w/v) trichloroacetic acid and analysed by western blotting using antibodies against caspase-3 or PARP-1. Activated forms of caspase-3 (p21, p19, p17) and truncated form of PARP-1 (tPARP-1) are indicated. (B) Both caspase-3 and PARP are negligibly processed upon H_2O_2 treatment. Cells were treated with 500 μM H_2O_2 for indicated times. Each reaction was stopped with 10% (w/v) trichloroacetic acid and analysed by western blotting as described in (A). The single and double asterisks indicate the non-specific bands. (C) AIF knockdown experiments. Saos-2 cells were transfected with siRNAs (scramble or AIF) as described in 'Experimental Procedures' section. Cells were then collected and subjected to SDS–PAGE followed by western blotting analysis using antibodies against AIF or actin. (D) H_2O_2-induced cell death is effectively suppressed by AIF knockdown. Saos-2 cells transfected with siRNAs were treated with 500 μM H_2O_2 for 48 h. Cell viability was then measured by trypan blue exclusion assay ($n = 10$). The asterisk ** indicates $P < 0.01$.

In MTS-P5 cells release of intramitochondrial cell death-inducing factors are suppressed

Next, we examined whether H_2O_2-induced cell death induces the release of intramitochondrial death-inducing factors in the MTS-P5 cells or not. First, we found that using immunofluorescence microscopy the release of cytochrome *c* (Fig. 6A), Smac/DIABLO (Supplementary Fig. S5A), HtrA2/Omi (Supplementary Fig. S5B) and AIF (Fig. 6C) was suppressed, which was also indicated by the largely consistent distribution patterns of fluorescence intensity (Fig. 6B and D). Similar results were also obtained with the cell fractionation experiments (Fig. 6E). Preliminary data indicate that upon H_2O_2 treatment polyADP-ribosylated smear bands were still observed in MTS-P5 cells (data not shown), suggesting that inhibition of PARP activity may not be required for the suppression and/or that acceptor proteins of poly(ADP-ribose) may be different in MTS-P5 cells from those of wild-type Saos-2 cells.

In MTS-P5 cells citrate synthase activity is protected against H_2O_2

Because in many cell deaths mitochondrial inner membrane potential ($\Delta\Psi m$) is declined as the death programme progresses, we next checked whether such dissipation is also suppressed in the MTS-P5 cells using JC-1, a lipophilic, cationic dye as a probe that can selectively enter mitochondria and reversibly changes colour from green to red as the $\Delta\Psi m$ increases (*34*). As shown in Supplementary Fig. S6, not only in Saos-2 cells, but also in the MTS-P5 cells, the $\Delta\Psi m$ was dissipated to a similar extent. Next, we examined whether intramitochondrial superoxide generation is suppressed or not, using fluorescent dye MitoSOX, which permeates live cells and selectively targets mitochondria, where it is rapidly oxidized by superoxide but not by other reactive oxygen or nitrogen species. As shown in Supplementary Fig. S7 left panels, in wild-type Saos-2 cells upon H_2O_2 treatment more intensely fluoresced cells appeared, suggesting

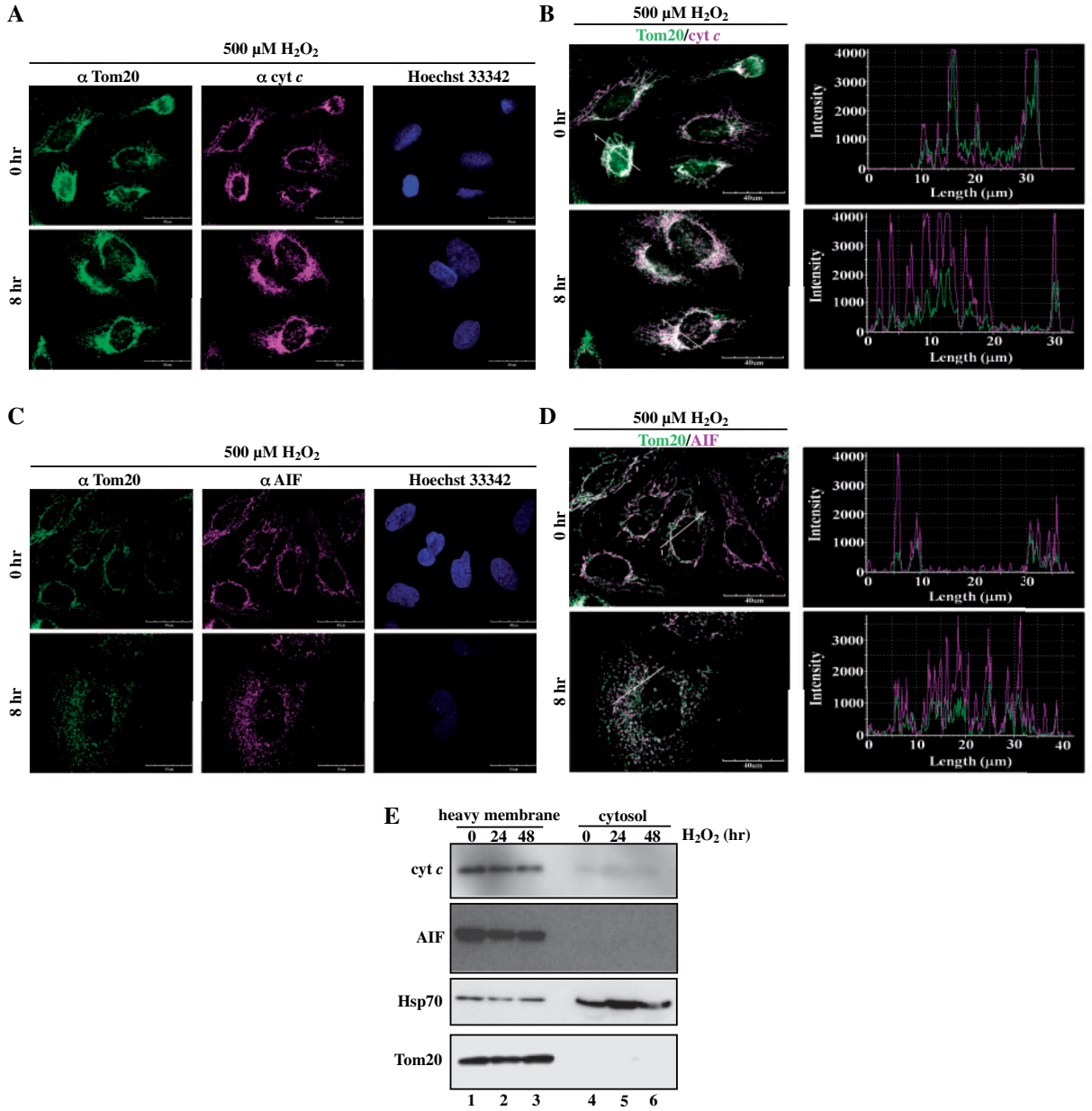

Fig. 6 H_2O_2-induced cell death is suppressed in MTS-P5 cells. Cells were treated and stained using antibodies against Tom20, cyt *c* (A and B) and AIF (C and D), and with Hoechst 33342, then analysed their intracellular distribution (B and D) as indicated in the legend to Fig 4. Bar indicates 40 μm. (E) Cell death-inducing factors release is suppressed in MTS-P5 cells revealed by subfractionation following western blotting as described in the legend to Fig 4(E).

H_2O_2 induced intramitochondrial superoxide formation which could be suppressed in the presence of NAC. On the other hand, as shown in Supplementary Fig. S7 right panels, in MTS-P5 cells, significant distribution change was hardly observed in the presence or absence of NAC, suggesting that in MTS-P5 cells intramitochondrial superoxide formation is probably suppressed.

How mitochondrial P5 suppressed H_2O_2-induced cell death? To answer this question, we next performed co-immunoprecipitation experiments using anti-FLAG IgG-conjugated Protein A Sepharose. As shown in Fig. 7A, middle panel, in MTS-P5 cells the expressed FLAG-tagged protein was effectively precipitated. Under these conditions, we found that citrate synthase, the rate-limiting enzyme in the TCA cycle, was coprecipitated (Fig. 7A, left panel). This interaction is likely to be specific because β-subunit of FoF1-ATPase (F1β) was not coprecipitated (Fig. 7A right panel). Next, we examined expression levels of citrate synthase. As shown in Fig. 7B, expression levels of citrate synthase, as well as control protein PDI, were not significantly decreased with or without H_2O_2 treatment. Notably, citrate synthase expression level elevated significantly compared with that in Saos-2 cells, whereas that of PDI was almost constant. Under these conditions, we next examined citrate synthase activity under H_2O_2-treated conditions. As shown in Fig. 7C, in wild-type

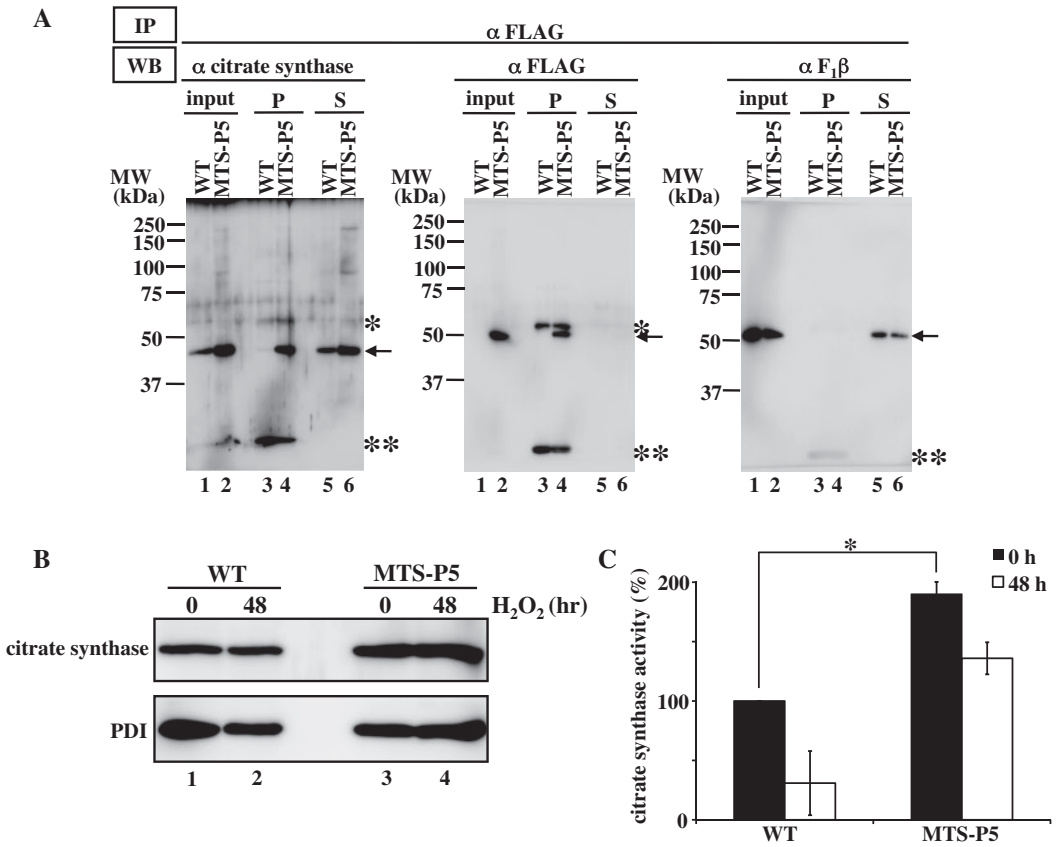

Fig. 7 Mitochondrial P5 interacts with citrate synthase to maintain its activity after H_2O_2 treatment. (A) Mitochondrial P5 coprecipitates with citrate synthase. Mitochondria isolated from wild-type Saos-2 (WT) and MTS-P5 cells were cross-linked, lysed and performed immunoprecipitation as described in section 'Experimental Procedures'. Each sample was subjected to western blotting using antibodies against citrate synthase (left panel), FLAG (middle panel), and F1β (right panel). Lanes 1 and 2, input fraction subjected to immunoprecipitation; lanes 3 and 4, immunoprecipitated pellet fraction; lanes 5 and 6, supernatant fraction after centrifugation. The single and double asterisks indicate the immunoglobulin heavy chain and light chain, respectively. (B) Expression levels of citrate synthase. Homogenates obtained from Saos-2 (WT) and MTS-P5 cells which had been treated with or without 500 μM H_2O_2 for 0 (Lanes 1 and 3) or 48 (Lanes 2 and 4) h were subjected to SDS–PAGE followed by western blotting using antibodies against citrate synthase or PDI. (C) Citrate synthase activity was almost maintained in MTS-P5 cells upon H_2O_2 treatment. Mitochondria were isolated from Saos-2 (WT) and MTS-P5 cells that had been treated with or without 500 μM H_2O_2 for 0 or 48 h and citrate synthase activity was measured as described in 'Experimental Procedures' section. Data are shown by mean ± SD ($n = 5$). The asterisk indicates $P < 0.05$.

Saos-2 cells the activity was significantly depressed upon H_2O_2 treatment, whereas in the MTS-P5 cells the large portion (~80%) of it was maintained even after 48 h with the treatment. These results are intriguing because previous report indicated that P5 exhibits molecular chaperone activity towards citrate synthase *in vitro* (*4*). Taken together, we conclude that mitochondrial P5 protects citrate synthase against H_2O_2 stress, probably through its chaperone activity.

Discussion

It has been thought that most PDI family proteins localize only in the ER. However, recent studies show that they reside also in the compartments outside the ER (*35*). P5, one of the PDI family members, has been reported to be secreted to the cell surface or to reside in mitochondria (*8*, *36*). To investigate the physiological function(s) of mitochondrial P5, we have characterized MTS-P5 cells that stably express P5 in mitochondria, and revealed that oxidative stress-induced cell death was suppressed in MTS-P5 cells. Our studies also showed that in Saos-2 cells H_2O_2-induced cell death was mediated largely through PARP-dependent and caspase-independent pathway, consistent with previous report (*28*). In that report, alkylating agent *N*-methyl-*N'*-nitro-*N*-nitrosoguanidine (MNNG) or H_2O_2 potentiates PARP activity, induces MOMP to release cytochrome *c* and AIF, eventually leading to cell death. Among released factors, AIF is likely to be an important death executioner, because AIF knockout (*28*) or knockdown (Fig. 5D, ref. *30*) significantly lowered the induced death. However, our results are apparently inconsistent with previous results in two points: AIF is released less extensively and more slowly compared with previous reports (*28*, *30*), and calpain activity is likely not to be required. For the former, these may be because some other factor(s) lacking in Saos-2 cells are required for efficient AIF release. One such candidate is p53, since Saos-2 cells are reported to be p53-null and in some cases p53 directly or indirectly activates Bax/Bak to induce MOMP (*37*, *38*). Another potential factor is mitochondrial ERK, because in the previous report ERK protects several cancer cells, including Saos-2 cells, against death through inhibition of the

permeability transition (*39*). Indeed, we have shown that Saos-2 cells are not very sensitive to stress stimuli (Fig. 2), possibly due to these cell-protecting factors. For the latter, although our results are not conclusive, we think it less likely that calpain(s) are required for the AIF release, because cell death was neither sensitive to calpain inhibitor (MDL28170) nor to z-VAD.fmk, which can inhibit not only caspases but also calpains. Whether calpain activation is required for AIF release is still a matter of debate (*30*, *40*) and further investigation are needed to clarify this point. Notably, we do not exclude the possibility that some other factor(s) other than AIF are required in order to induce H_2O_2-induced cell death, and further investigations are required to elucidate these issues.

How is the oxidative stress-induced cell death suppressed in the MTS-P5 cells? To answer this question, we performed a series of experiments and have revealed that the release of intramitochondrial death-inducing factors, including AIF, was suppressed, while H_2O_2-induced polyADP-ribosylation was not significantly suppressed. In relation to this, recent studies show that free poly(ADP-ribose) (PAR) resulting from PARP activation directly binds to AIF on the mitochondrial outer membrane to cause its release (*41–43*). How do these facts reconcile with our present data? Since mitochondrial P5 is likely not to act on PAR generation and since dissipation of $\Delta\Psi m$, probably resulting from acting of free PAR to mitochondria (*28*, *41*), is similarly observed in MTS-P5 cells, mitochondrial P5 may prevent PAR binding to AIF, probably indirectly. So one possibility is that ROS-dependent posttranslational modification on AIF is required for efficient PAR binding, considering together that intramitochondrial superoxide generation is suppressed in the MTS-P5 cells. However, we think this less likely, because the release suppression is not specific to AIF and so far it has not been reported for direct stimulatory effect(s) of PAR on MOMP.

Another possibility is that some other factor(s) derived from mitochondria in the MTS-P5 cells prevent, directly or indirectly, the AIF release. As shown in this study, we have identified citrate synthase, the rate-limiting enzyme of the TCA cycle, as one of possible target proteins of mitochondrial P5. This interaction is likely to be relevant because significant portions of its activity were maintained after 48 h upon H_2O_2 treatment. Since even under healthy state in MTS-P5 cells the expressed level of citrate synthase elevated around 1.5-fold, it is plausible that the levels of some intermediate molecule(s) of TCA cycle are also elevated. Indeed mitochondrial NADH level in MTS-P5 cells are found to be elevated compared to with that in control Saos-2 cells (Y. Shitara *et al.*, unpublished data). Intriguingly, enough, recent reports have shown that some TCA cycle-derived metabolites (succinate, fumarate, citrate, etc.) resulting from proliferating or oncogenic metabolism upregulate amino acid and lipid biosynthesis, or associate with transcriptional regulation (hypoxia-inducible factor-1, histone demethylases, etc.), or are utilized as an antioxidant (*44–49*). On the basis of these results, we speculate that mitochondrial P5 could upregulate mitochondrial metabolism, including TCA cycle, thereby preventing the death pathway through TCA cycle-derived metabolite-dependent mechanism.

Another important issue remained to be solved is to elucidate physiological function(s) of mitochondrial P5. Indeed, in Saos-2 cells that endogenous P5 had been knocked down, H_2O_2-induced cell death was not significantly increased compared to that in control cells, while in MTS-P5 cells that had been similarly treated, cell viability was significantly lowered (Y. Shitara *et al.*, unpublished data). At present, we speculate that mitochondrial P5 would exhibit activities of suppressing cell death in such condition(s) that might overexpress mitochondrial P5, for example, the unfolded protein response. Mitochondrial P5 could also have a role other than the cell death signalling. Previously it was shown that the isomerase and chaperone activities are weaker than those of PDI (*4*). However, P5 possesses a function that PDI does not have. For example, expression of P5 in the embryonic midline has been reported to be required for the establishment of left/right asymmetries during ontogeny (*50*). Furthermore, in contrast to our results, recent report indicates that PDI stimulates apoptosis induced by misfolded proteins through triggering MOMP (*51*). Thus, physiological function(s) of P5 are likely to be differentiated from those of PDI, and its dual localization may be the reason for such functional diversity. We have suggested three possibilities for the physiological significance of P5 in mitochondria (*8*): (i) as an oxidoreductase, (ii) as an assembly factor or a chaperone or (iii) as yet unidentified activities. In this study, we have shown that mitochondrial P5 is in close contact with citrate synthase and protect its enzyme activity against oxidative stress. This is probably due to P5 chaperone activity described previously, although the mechanism underlying this protection requires further investigation (*4*).

Taken together, future studies, including the identification of additional interacting proteins in mitochondria, the extensive analysis with metabolic or gene expression change(s) and the elucidation of cell death suppression mechanism, will pave the way to elucidate not only unique function(s) of P5, but also relationships between mitochondrial energy metabolism and cell death pathway.

Supplementary Data

Supplementary Data are available at *JB* Online.

Acknowledgements

We are grateful to Drs Akitsugu Yamamoto (NIBST) and Tomohisa Horibe (Kyoto University) for critical reading of the manuscript, and to Drs Kazuo Kamemura (NIBST), Atsuki Nara (NIBST) and Chieri Ida (NIBST) for helpful experimental support and discussion.

Conflict of interest
None declared.

References

1. Ferrari, D.M. and Soling, H.-D. (1999) The protein disulphide-isomerase family: unraveling a string of folds. *Biochem. J.* **339**, 1–10
2. Appenzeller-Herzog, C. and Ellgaard, L. (2008) The human PDI family: Versatility packed into a single fold. *Biochim. Biophys. Acta* **1783**, 535–548
3. Rupp, K., Birnbach, U., Lundstrom, J., Van, P.-N., and Soling, H.-D. (1994) Effects of CaBP2, the Rat Analog of ERp72, and of CaBP1 on the refolding of denatured reduced proteins. *J. Biol. Chem.* **269**, 2501–2507
4. Kikuchi, M., Doi, E., Tsujimoto, I., Horibe, T., and Tsujimoto, Y. (2002) Functional analysis of human P5, a protein disulfide isomerase homologue. *J. Biochem.* **132**, 451–455
5. Rutkevich, L.A., Cohen-Doyle, M.F., Brockmeier, U., and Williams, D.B. (2010) Functional relationship between protein disulfide isomerase family members during the oxidative folding of human secretory proteins. *Mol. Biol. Cell* **21**, 3093–3105
6. Jessop, C.E., Watkins, R.H., Simmons, J.J., Tasab, M., and Bulleid, N.J. (2010) Protein disulphide isomerase family members show distinct substrate specificity: P5 is targeted to BiP client proteins. *J. Cell Sci.* **122**, 4287–4295
7. Fullekrug, J., Sonnichsen, B., Wunsch, U., Arseven, K., Van, P.-N., Soling, H.-D., and Mieskes, G. (1994) CaBP1, a calcium binding protein of the thioredoxin family, is a resident KDEL protein of the ER and not of the intermediate compartment. *J. Cell Sci.* **107**, 2719–2727
8. Kimura, T., Horibe, T., Sakamoto, C., Shitara, Y., Fujiwara, F., Komiya, T., Yamamoto, A., Hayano, T., Takahashi, N., and Kikuchi, M. (2008) Evidence for mitochondrial localization of P5, a member of the protein disulphide isomerase family. *J. Biochem.* **144**, 187–196
9. Tait, S.W.G. and Green, D.R. (2010) Mitochondria and cell death: outer membrane permeabilization and beyond. *Nat. Rev. Mol. Cell Biol.* **11**, 621–632
10. Degterev, A. and Yuan, J. (2008) Expansion and evolution of cell death programmes. *Nat. Rev. Mol. Cell Biol.* **9**, 378–390
11. Vanlangenakker, N., Berghe, T.V., and Vandenabeele, P. (2012) Many stimuli pull the necrotic trigger, an overview. *Cell Death Diff.* **19**, 75–86
12. Veal, E.A., Day, A.M., and Morgan, B.A. (2007) Hydrogen peroxide sensing and signaling. *Mol. Cell* **26**, 1–14
13. Giorgio, M., Trinei, M., Migliaccio, E., and Pelicci, P.G. (2007) Hydrogen peroxide: a metabolic by-product or a common mediator of aging signals? *Nat. Rev. Mol. Cell Biol.* **8**, 722–728
14. Finkel, T. (2011) Signal transduction by reactive oxygen species. *J. Cell Biol* **194**, 7–15
15. Circu, M.L. and Aw, T.Y. (2010) Reactive oxygen species, cellular redox systems, and apoptosis. *Free Rad. Biol. Med.* **48**, 749–762
16. Troyano, A., Sancho, P., Fernandez, C., de Blas, E., Bernardi, P., and Aller, P. (2003) The selection between apoptosis and necrosis is differentially regulated in hydrogen peroxide-treated and glutathione-depleted human promonocytic cells. *Cell Death Diff.* **10**, 889–898
17. Reardon, J.T., Bessho, T., Kung, H.C., Bolton, P.H., and Sancar, A. (1997) *In vitro* repair of oxidative DNA damage by human nucleotide excision repair system: possible explanation for neurodegeneration in xeroderma pigmentosum patients. *Proc. Natl. Acad. Sci. USA* **94**, 9463–9468
18. Schreiber, V., Dantzer, F., Ame, J.-C., and de Murcia, G. (2006) Poly(ADP-ribode): novel functions for an old molecule. *Nat. Rev. Mol. Cell Biol.* **7**, 517–528
19. Heeres, J.T. and Hergenrother, P.J. (2007) Poly(ADP-ribose) makes a date with death. *Curr. Opin. Chem. Biol.* **11**, 644–653
20. Higuchi, M., Proske, R.J., and Yeh, E.T.H. (1998) Inhibition of mitochondrial respiratory chain complex I by TNF results in cytochrome *c* release, membrane permeability transition, and apoptosis. *Oncogene* **17**, 2515–2524
21. Li, N., Ragheb, K., Lawler, G., Sturgis, J., Rajwa, B., Melendez, J.A., and Robinson, J.P. (2003) Mitochondrial complex I inhibitor rotenone induces apoptosis through enhancing mitochondrial reactive oxygen species production. *J. Biol. Chem.* **278**, 8516–8525
22. Chen, Y., McMillan-Ward, E., Kong, J., Israels, S.J., and Gibson, S.B. (2007) Mitochondrial electron-transport-chain inhibitors of complexes I and II induce autophagic cell death mediated by reactive oxygen species. *J. Cell Sci.* **120**, 4155–4166
23. Choi, W.-S., Palmiter, R.D., and Xia, Z. (2011) Loss of mitochondrial complex I activity potentiates dopamine neuron death induced by microtubule dysfunction in a Parkinson's disease model. *J. Cell Biol.* **192**, 873–882
24. Tiwari, M., Lopez-Cruzan, M., Morgan, W.W., and Herman, B. (2011) Loss of caspase-2-dependent apoptosis induces autophagy after mitochondrial oxidative stress in primary cultures of young adult cortical neurons. *J. Biol. Chem.* **286**, 8493–8506
25. Zhou, C., Huang, Y., Shao, Y., May, J., Prou, D., Perier, C., Dauer, W., Schon, E.A., and Przedborski, S. (2008) The kinase domain of mitochondrial PINK1 faces the cytoplasm. *Proc. Natl. Acad. Sci. USA* **105**, 12022–12027
26. Kawamitsu, H., Hoshino, H., Okada, H., Miwa, M., Momoi, H., and Sugimura, T. (1984) Monoclonal antibodies to poly(adenosine diphosphate ribose) recognize different structures. *Biochemistry* **23**, 3771–3777
27. Shapovalov, Y., Hoffman, D., Zuch, D., de Mesy Bentley, K.L., and Eliseev, R.A. (2011) Mitochondrial dysfunction in cancer cells due to aberrant mitochondrial replication. *J. Biol. Chem.* **286**, 22331–22338
28. Yu, S.W., Wang, H., Poitras, M.F., Coombs, C., Bowers, W.J., Federoff, H.J., Poirier, G.G., Dawson, T.M., and Dawson, V.L. (2002) Mediation of poly(ADP-ribose) polymerase-1-dependent cell death by apoptosis-inducing factor. *Science* **297**, 259–263
29. Degterev, A., Hitomi, J., Germsceid, M., Ch'en, I.L., Korkina, O., Teng, X., Abbott, D., Cuny, G.D., Yuan, C., Wagner, G., Hedrick, S.M., Gerber, S.A., Lugovskoy, A., and Yuan, J. (2008) Identification of RIP1 kinase as a specific cellular target of necrostatins. *Nat. Chem. Biol.* **4**, 313–321
30. Moubarak, R.S., Yuste, V.J., Artus, C., Bouharrour, A., Greer, P.A., Menissier-de Murcia, J., and Susin, S.A. (2007) Sequential activation of poly(ADP-ribose) polymerase 1, calpains, and Bax is essential in apoptosis-inducing factor-mediated programmed necrosis. *Mol. Cell. Biol.* **27**, 4844–4862
31. Cilenti, L., Lee, Y., Hess, S., Srinivasula, S., Park, K.M., Junqueira, D., Davis, H., Bonventre, J.V., Alnemri, E.S., and Zervos, A.S. (2003) Characterization of a novel and

specific inhibitor for the pro-apoptotic protease Omi/HtrA2. *J. Biol. Chem.* **278**, 11489–11494

32. Suzuki, Y., Imai, Y., Nakayama, H., Takahashi, K., Takio, K., and Takahashi, R. (2001) A serine protease, HtrA2, is required from the mitochondria and interacts with XIAP, inducing cell death. *Mol. Cell* **8**, 613–621
33. Hegde, R., Srinivasula, S.M., Zhang, Z.J., Wassell, R., Mukattash, R., Cilenti, L., DuBois, G., Lazebnik, Y., Zervos, A.S., Fernandes-Alnemri, T., and Alnemri, E.S. (2002) Identification of Omi/HtrA2 as a mitochondrial apoptotic serine protease that disrupts inhibitor of apoptosis protein-caspase interaction. *J. Biol. Chem.* **277**, 432–438
34. Reers, M., Smith, T.W., and Chen, L.B. (1991) J-aggregate formation of a carbocyanine as a quantitative fluorescent indicator of membrane potential. *Biochemistry* **30**, 4480–4486
35. Turano, C., Coppari, S., Altieri, F., and Ferraro, A. (2002) Proteins of the PDI family: unpredicted non-ER locations and functions. *J. Cell. Phys.* **193**, 154–163
36. Kaiser, B.K., Yim, D., Chow, I.T., Gonzalez, S., Dai, Z., Mann, H.H., Strong, R.K., Groh, V., and Spies, T. (2007) Disulphide-isomerase-enabled shedding of tumour-associated NKG2D ligands. *Nature* **447**, 482–486
37. Marcellus, R.C., Teodoro, J.G., Charbonneau, R., Shore, G.C., and Branton, P.E. (1996) Expression of p53 in Saos-2 osteosarcoma cells induces apoptosis which can be inhibited by Bcl-2 or the adenovirus E1B-55 kDa protein. *Cell Growth Diff.* **7**, 1643–1650
38. Lindenboim, L., Borner, C., and Stein, R. (2011) Nuclear proteins acting on mitochondria. *Biochim. Biophys. Acta* **1813**, 584–596
39. Rasola, A., Sciacovelli, M., Chiara, F., Pantic, B., Brusilow, W.S., and Bernardi, P. (2010) Activation of mitochondrial ERK protects cancer cells from death through inhibition of the permeability transition. *Proc. Natl. Acad. Sci. USA* **107**, 726–731
40. Modjtahedi, N., Giordanetto, F., Madeo, F., and Kroemer, G. (2006) Apoptosis-inducing factor: vital and lethal. *Trends Cell Biol.* **16**, 264–272
41. Yu, S.W., Andrabi, S.A., Wang, H., Kim, N.S., Poirier, G.G., Dawson, T.M., and Dawson, V.L. (2006) Apoptosis-inducing factor mediates poly(ADP-ribose) (PAR) polymer-induced cell death. *Proc. Natl. Acad. Sci. USA* **103**, 18314–18319
42. Yu, S.W., Wang, Y., Frydenlund, D.S., Ottersen, O.P., Dawson, V.L., and Dawson, T.M. (2009) Outer mitochondrial membrane localization of apoptosis-inducing factor: mechanistic implications for release. *ASN Neuro* **1**, e00021
43. Wang, Y., Kim, N.S., Haince, J.-F., Kang, H.C., David, K.K., Andrabi, S.A., Poirier, G.G., Dawson, V.L., and Dawson, T.M. (2011) Poly(ADP-ribose) (PAR) binding to apoptosis-inducing factor is critical for PAR polymerase-1-dependent cell death (Parthanatos). *Sci. Signal.* **4**, ra20
44. DeBerardinis, R.J., Lum, J.J., Hatzivassiliou, G., and Thompson, C.B. (2008) The biology of cancer: metabolic reprogramming fuels cell growth and proliferation. *Cell Metab.* **7**, 11–20
45. Teperino, R., Schoonjans, K., and Auwerx, J. (2010) Histone methyl transferases and demethylases; can they link metabolism and transcription? *Cell Metab.* **12**, 321–327
46. Buchakjian, M.R. and Kornbluth, S. (2010) The engine driving the ship: metabolic steering of cell proliferation and death. *Nat. Rev. Mol. Cell Biol.* **11**, 715–727
47. Raimundo, N., Baysal, B.E., and Shadel, G.S. (2011) Revisiting the TCA cycle: signaling to tumor formation. *Trends Mol. Med.* **17**, 641–649
48. Icard, P., Poulain, L., and Lincet, H. (2012) Understanding the central role of citrate in the metabolism of cancer cells. *Biochim. Biophys. Acta* **1825**, 111–116
49. Mailloux, R.J., Beriault, R., Lemire, J., Singh, R., Chenier, D.R., Hamel, R.D., and Appanna, V.D. (2007) The tricarboxylic acid cycle, an ancient metabolic network with a novel twist. *PLoS ONE* **2**, e690
50. Hoshijima, K., Metherall, J.E., and Grunwald, D.J. (2002) A protein disulfide isomerase expressed in the embryonic midline is required for left/right assymmetries. *Genes & Dev.* **16**, 2518–2529
51. Hoffstrom, B.G., Kaplan, A., Letso, R., Schmid, R.S., Turmel, G.J., Lo, D.C., and Stockwell, B.R. (2010) Inhibitors of protein disulfide isomerase suppress apoptosis induced by misfolded proteins. *Nat. Chem. Biol.* **6**, 900–906